

Mapping of the mouse *hyh* gene to a YAC/BAC contig on proximal Chromosome 7

Teresa H. Chae,^{1,*} Kristina M. Allen,^{1,***} Muriel T. Davisson,² Hope O. Sweet,² Christopher A. Walsh¹

¹Dept. of Neurology, Beth Israel Deaconess Medical Center, Harvard Institutes of Medicine, Room 816, 77 Avenue Louis Pasteur, Boston, Massachusetts 02115, USA

²The Jackson Laboratory, Bar Harbor, Maine 04609-1500, USA

Received: 22 October 2001 / Accepted: 10 January 2002

Abstract. Mice that are homozygous for the autosomal recessive hydrocephaly with hop gait (*hyh*) mutation on Chromosome (Chr) 7 have congenital hydrocephalus characterized by an interhemispheric cyst arising from the third ventricle and agenesis of the corpus callosum. Analysis of more than 500 backcross and intercross progeny maps the *hyh* locus to proximal Chr 7, approximately 13 cM centromeric to its originally reported map position. Analysis of recombinants at several MIT microsatellite markers localized the *hyh* locus between *D7Mit75* and *D7Mit56*. Development of several new SSLP markers allowed us to refine the *hyh* candidate interval to a region defined by the cone-rod homeobox (*Crx*) gene proximally and *D7Mit56* distally. A contig of yeast artificial chromosome (YAC) clones and bacterial artificial chromosome (BAC) clones spanning this entire region has been developed, and a number of potential candidate genes for *hyh* within this interval have been identified. Gene content is conserved between this region of mouse Chr 7 and human Chr 19q13.3. Physical mapping of the regions around *D7Mit75* and *D7Mit56* has also determined the order of a number of MIT markers that remain unresolved on the Mouse Genome Database (MGD) map. Our physical map and transcript map may be useful for positional cloning of genes in this unusually gene-rich region of the genome.

The mouse mutant hydrocephalus with hop gait (*hyh*) is one in a series of spontaneous mouse mutants with autosomal recessive forms of hydrocephalus (Bronson and Lane 1990). Several of these hydrocephalic mice show otherwise normal brain development. However, in other hydrocephalic mice, including congenital hydrocephalus (*Foxc1^{ch}*) (Green 1970; Kume et al. 1998), hydrocephalic-polydactyly (hop^{hpy}) (Hollander 1976), hydrocephalus 1 (*hy1*) (Clark 1932), and *hyh*, the hydrocephalus reflects a widespread developmental anomaly of the brain. These mouse mutants may represent important animal models for human congenital hydrocephalus, which is etiologically heterogeneous, but also define genes required for normal brain patterning.

The most striking aspect of the *hyh* phenotype is the dramatic cystic dilation of the third ventricle and dilatation of the lateral ventricles and caudal aqueduct that are present at birth and progressively worsen with age (Bronson and Lane 1990). In humans, hydrocephalus is rarely caused by overproduction of cerebrospinal fluid (CSF), but rather by blockage of CSF flow. Interestingly, in

the *hyh* mouse there appears to be no blockage of CSF flow within the ventricular system at birth, although there is extensive expansion of the ventricles (Perez-Figares et al. 1998). Therefore, the exact etiology of the hydrocephalus is still uncertain.

Extensive ependymal denudation has been observed during embryogenesis prior to expansion of the ventricles (Jimenez et al. 2001). The third ventricular cyst eventually displaces other midline structures and extends between the cerebral hemispheres. Worsening hydrocephalus leads to doming of the head and probably is responsible for lethality within weeks to a few months after birth. Other abnormalities of note are the failure of corpus callosum fibers to cross the midline, instead forming Probst bundles on either side of the expanded third ventricle, disorganization of neurons in the rostral vermis of the cerebellum (Bronson and Lane 1990), and complete absence of the central canal of the spinal cord (Perez-Figares et al. 1998).

We have undertaken the genetic and physical mapping of the *hyh* gene. The *hyh* gene was originally mapped to about 15.2 cM from the centromere of Chr 7 on the basis of intercrosses with 80 meioses, by using visible and electrophoretic markers (Bronson and Lane 1990). We have localized *hyh* more precisely to proximal Chr 7, approximately 13 cM away from its originally reported location. A complete YAC/BAC contig of this region has been generated, and a number of candidate genes for *hyh* have been identified, establishing conservation between the *hyh* candidate interval and human Chr 19q13.3, one of the most gene-rich regions of the human genome (Lander et al. 2001; Venter et al. 2001). Our physical mapping has also ordered a number of MIT markers that remain unresolved on the Mouse Genome Database map (MGD 2001) and has generated several new polymorphic microsatellite markers. These data should be useful to other researchers undertaking positional cloning of genes on proximal Chr 7.

Materials and methods

Animals and matings. Mice were obtained from The Jackson Laboratory (Bar Harbor, Me.) where the *hyh* mutation originally arose in the C57BL/10J inbred strain and was subsequently placed on a B6C3Fe-*a/a* (C57BL/6J female × C3HeB/FeJ-*a/a* male) hybrid background by alternately crossing transplanted ovaries from *hyh/hyh* females to B6C3Fe F₁ hybrid males and intercrossing the obligate heterozygous progeny (Bronson and Lane 1990). Since the *hyh* mutation arose on the C57BL/10J background, the mutation should segregate with the C57BL/10J alleles of closely linked markers. Therefore, mice from the maintenance cross determined to be heterozygous for C57BL/10J and C3HeB/FeJ-*a/a* alleles at the markers *D7Mit75*, *56*, *76*, and *57* and determined to be heterozygous for the *hyh* mutation were intercrossed to produce the F₂ progeny or were mated to the ovary-transplanted *hyh/hyh* female to produce the backcross progeny analyzed in this report. Mice were housed and handled in accordance with protocols approved by the IACUC of Harvard Medical School.

Correspondence to: C.A. Walsh; E-mail: cwalsh@caregroup.harvard.edu

*These authors contributed equally to this work.

**Present address: Genome Therapeutics Corporation, 100 Beaver Street, Waltham, MA 02453-8443, USA.

Assessment of *hyh* genotype. Homozygous mutant mice were identified either by their grossly visible dome-shaped head and hopping gait by 3 weeks of age and/or by histologic analysis for an interhemispheric cyst. Heterozygous mice were identified by their ability to produce homozygous affected progeny when bred to known heterozygotes.

Microsatellite testing. DNA was obtained from tail clippings of 3- to 4-week-old mice; tail tips were then digested for 12–16 h with Proteinase K in 0.2 ml PBD (50 mM KCl, 10 mM Tris pH 8, 2.5 mM MgCl₂, 0.1 mg/ml gelatin, 0.45% vol/vol NP40, 0.45% Tween 20, 50 µg/ml Proteinase K). Primers for microsatellite markers were purchased from Research Genetics (Huntsville, Ala.). PCR was performed with the PTC-100 Thermal Cycler (MJ Research, Waltham, Mass.) after end-labeling of primers with $\gamma^{32}\text{P}$ -ATP using tail digest as template. Denatured samples were subjected to electrophoresis on a 5% acrylamide gel (36% urea, 1× TBE) at 55°C, which was then fixed, dried, and exposed to film overnight. Alternatively, non-radioactively labeled PCR products were subjected to electrophoresis on a denaturing 5% acrylamide gel as described above and stained with SILVER SEQUENCE™ Staining Reagents (Promega, Madison, WI) according to the manufacturer's specifications to visualize DNA.

Identification of YAC clones. The Whitehead I Mouse YAC library (Research Genetics) was screened for clones containing relevant microsatellite markers by PCR. Additional YAC clones containing markers of interest were identified from the Mouse Genomic Mapping Project data (Nusbaum et al. 1999) available on the internet at www-genome.wi.mit.edu/cgi-bin/mouse/index. These clones from the WI/MIT-820 Mouse YAC library were obtained from Research Genetics.

Screening of BAC libraries. The CITB mouse BAC library (Research Genetics) was screened by PCR and by hybridization according to the supplier's instructions. The RPCI-23 mouse BAC library (Research Genetics) was obtained on high-density filters and screened by hybridization with radioactive probes in aqueous hybridization solution as described (Ausubel et al. 1995).

Sequencing of BAC ends. BAC end sequences were obtained through vectorette PCR and sequencing of the resulting PCR products as previously described (Ware et al. 1997) with minor modifications. Primers were designed against BAC vector sequence adjacent to the insert cloning sites. For CITB clones (pBeloBac11 vector) the primer sequences are: forward primer 5'CGACTCACTATAGGGCGAATTC and reverse primer 5'CG-GCTCGTATGTTGTGTGGA. For RPCI-23 clones (pBACe3.6 vector) the primer sequences are: forward primer 5'GAAGGAGCTGACTGGGTTGA and reverse primer 5'CGATCCTCCCAATTGACTA. PCR products were subsequently gel-purified with the GeneClean Kit (Qbiogene, Carlsbad, Calif.), sequenced by using the ABI Big Dye Cycle Sequencing Kit, and analyzed on an ABI 377 Sequencer (Applied Biosystems, Foster City, Calif.). BAC end sequences were screened for repetitive elements with RepeatMasker (Smit and Green 2000), and primers were designed using Primer3 (Rozen and Skaletsky 1998) to produce products 150–500 bp in length. STSs designed from BAC end sequences are named by the clone address and either "F" or "R" depending on whether the sequence was obtained from PCR reactions using the forward or reverse primer, respectively, of the BAC vector.

Identification of genes within candidate interval. BAC DNA was prepared either by standard alkaline lysis miniprep (Ausubel et al. 1995) or using the BAC Large-Plasmid Purification Kit (Incyte Genomics, Palo Alto, Calif.). DNA was digested with *Eco*RI and *Hind*III or *Not*I and *Hind*III restriction enzymes and cloned into pBluescript SK- (Stratagene, La Jolla, Calif.). Clones were randomly selected and sequenced from T7 and T3 primers with the ABI Big Dye Cycle Sequencing Kit and ABI 377 Sequencer (Applied Biosystems). Sequences were screened for repetitive elements using RepeatMasker (Smit and Green 2000) and then analyzed by BLAST (Altschul et al. 1997) for sequence corresponding to known genes or for similarity to mouse genome draft sequence. Mouse genomic sequence identified by BLAST was analyzed using the same methods to identify known genes. Primers to genes identified in this manner were then used to confirm their presence in the contig by PCR with the exception of *Kiaa1064*, which was confirmed by Southern blot analysis with the insert

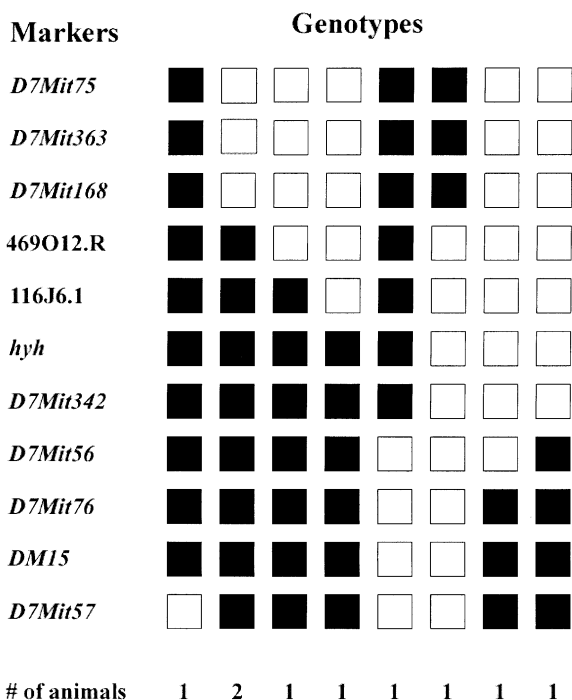


Fig. 1. Genetic mapping of the *hyh* locus. A subset of backcross and intercross progeny with recombination events between *D7Mit75* and *D7Mit57* and of known genotype at the *hyh* locus were genotyped at a number of additional markers. Black boxes indicate homozygosity for the C57BL/10J allele, and white boxes indicate heterozygosity for the C57BL/10J and C3HeB/FeJ-*a/a* alleles.

of IMAGE cDNA clone 420741 (Research Genetics), a mouse cDNA highly homologous to the 3' end of human KIAA1064, as a probe.

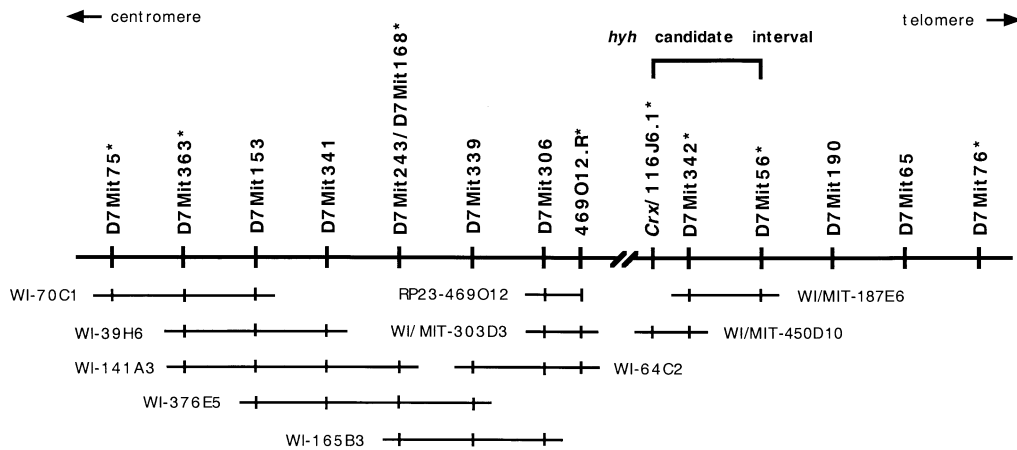
Results

***hyh* maps proximal to *Gpi1*.** Several homozygous mutant mice were initially genotyped for markers spanning the proximal 40 cM of Chr 7. Since the *hyh* mutation arose on the C57BL/10J background, the *hyh/hyh* homozygous mutants should be homozygous for the C57BL/10J alleles of closely linked markers even though *hyh* is now maintained on a B6C3Fe-*a/a* genetic background. Only those markers on proximal Chr 7, extending from *D7Mit75* proximally through *D7Mit57* distally, consistently segregated with *hyh*. Those markers that flank the originally published map position distal to the glucose phosphate isomerase 1 (*Gpi1*) locus, *D7Mit25* and *D7Mit52*, as well as more distal markers, showed much greater recombination with *hyh*.

The *hyh* gene maps between *D7Mit75* and *D7Mit56*. Two initial recombinants from the backcross place *hyh* distal to *D7Mit75* and proximal to *D7Mit57*. Subsequently, a total of 81 backcross and 411 F₂ progeny were genotyped for four polymorphic microsatellite markers on proximal Chr 7, whose order from centromere to telomere is: *D7Mit75*, *D7Mit56*, *D7Mit76*, and *D7Mit57* (Fig. 1). Thirteen of 14 recombinants between *D7Mit75* and *D7Mit56* were of known genotype at the *hyh* locus. Of these 13 recombinants, 8 place *hyh* telomeric to *D7Mit75*, and 5 place *hyh* centromeric to *D7Mit56*. This initial genetic mapping localizes the *hyh* gene to a 1.55-cM interval on proximal Chr 7.

A subset of seven recombinants between *D7Mit75* and *D7Mit56* were genotyped at a number of additional microsatellite markers on proximal Chr 7: *D7Mit363* and *D7Mit168*, known to be

A



B

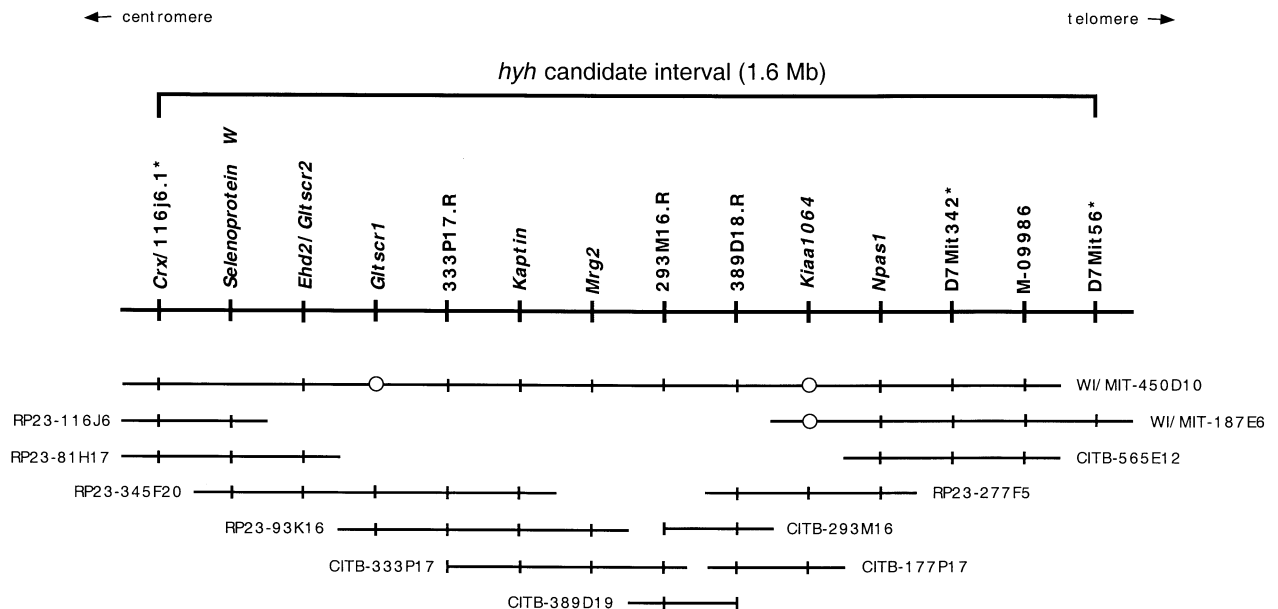


Fig. 2. Physical Mapping of the *hyh* locus. (A) YAC/BAC contig spanning *D7Mit75* and *D7Mit56*. (B) A more detailed view of the YAC/BAC contig spanning the *hyh* candidate interval. The upper line in each contig represents a region on Chr 7 with centromere to the left and telomere to the right and STSs indicated above. STSs whose order could not be resolved are listed together. Asterisks indicate STSs that are polymorphic between C57BL/10J and C3HeB/FeJ-*a/a*. YAC and BAC clones are indicated by

horizontal lines whose length is determined by STS content, not actual physical size. Vertical lines indicate STS content, and open circles indicate markers that have not been tested in a given clone. Letters preceding the YAC or BAC address indicate the library source: CITB, CITB Mouse BAC library; RP23, RPCI-23 Mouse BAC library; WI, Whitehead I Mouse YAC library; WI/MIT, WI/MIT820 Mouse YAC library.

polymorphic between C57BL/10J and C3HeB/FeJ-*a/a*, as well as *D7Mit342*, which was found to be polymorphic through our own analysis (Fig. 3). *D7Mit363* and *D7Mit168* were not separable from *D7Mit75* but were subsequently ordered and determined to be telomeric to *D7Mit75* through physical mapping. *D7Mit342*, however, was determined to be centromeric to *D7Mit56* and non-recombinant with *hyh* in the mice analyzed.

Localization of the hyh gene to a YAC/BAC contig spanning Crx to D7Mit56. In order to generate a physical map of the *hyh* candidate interval, a YAC/BAC contig anchored by *D7Mit75* and *D7Mit56* was constructed (Fig. 2a). A single discontinuity could not be

bridged. Construction of this contig resolves the physical order of a number of MIT markers: *D7Mit75*, *D7Mit363*, *D7Mit153*, *D7Mit341*, *D7Mit168/D7Mit243*, *D7Mit339* and *D7Mit306*. *D7Mit168* and *D7Mit243* cannot be resolved. The end sequence of BAC RP23-469O12 (469O12.R), which contains *D7Mit306*, was found to contain a SLP (Table 1, Fig. 3). Genotyping of recombinants at this marker revealed that it lies distal to *D7Mit75*, serving to orient the contig, and lies proximal to the *hyh* locus, thus excluding most of this contig from the *hyh* candidate interval (Fig. 1).

The more distal portion of the contig, containing *D7Mit56* and *D7Mit342*, minimally consists of two YACs (Fig. 2a). In addition, BACs extending proximally from *D7Mit342* were identified to

Table 1. Newly generated STSs.

STS	Forward Primer (5' → 3')	Reverse Primer (5' → 3')	Size (bp)
116J6.1 ^{a*}	AACAAAATACGACCCCTC	TCAGCCAGTAGGAAGGCTA	222
293M16.R ^b	CACAGTCTGCACCCTCTGAA	CAGAAGCAGCCACCATTACA	195
333P17.R ^c	TCCCCTCTACACCAAGCATT	CAGCATCCCAGGGTACCTAA	201
389D19.R ^d	GATTTGGCATAAAAGCCATCA	ACTGTACACAGGCACAAGC	208
469O12.R ^{e*}	ACCTTTCCGCCAGTGTGGATA	AGGTGGAGCAGAGGAACCTT	248
<i>Crx</i>	TTCCAGCGGAATCACTCTTT	GAAGGAGCCACTTTCATTGC	200
<i>Dm15</i> [*]	CAATGGGCTGAGCTCTCATCT	CCAAGACAGCCAGAGCTACA	230
<i>Ehd2</i>	ATGGCACATGACTTCACCAA	CCCTTCTGTCTGCTCGCTTAGA	530
<i>Gltscr1</i>	ACTGTACTGACCCACCAGGC	GAGTTCGCCGTGAGTGTGGT	395
<i>Gltscr2</i>	AGCTTGCAGCAGCTTTCT	GAGTCCGTGTTCCGGGAGAT	200
<i>Kaptn</i>	GGAGGAATTTAACCCCACTCA	CCCAAGGTGATGGAGTCACT	202
<i>Mrg2</i>	CGTACCCCTCAGAAGACAAA	CTATTCGTCTCCGGGCATTA	269
<i>Npas1</i>	CGCATCAAAGTGGAGGCC	CAACGGGTGGCAGGAAGC	155
<i>Sepw1</i>	TGGTCTTCTCCTGATGTTC	TCTTGAGGTGGAAAGGGAAA	191

* STS contains SSLP between the strains C57BL/10J and C3HeB/FeJ-*a/a*. See Fig 3.

^a GenBank accession number BH610087.

^b GenBank accession number BH610089.

^c GenBank accession number BH610090.

^d GenBank accession number BH610091.

^e GenBank accession number BH610088.

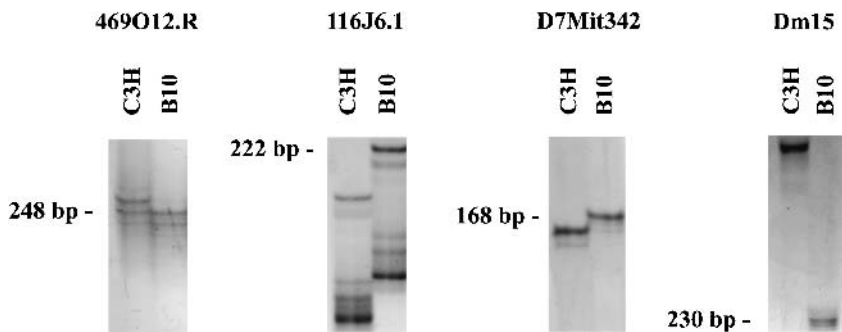


Fig. 3. Polymorphic microsatellite markers. Newly identified SLPs between C57BL/10J and C3HeB/FeJ-*a/a* are illustrated for *D7Mit342* and three newly identified STSs: 469O12.R, 116J6.1, and Dm15. C57BL/10J alleles are labeled as B10, and C3HeB/FeJ-*a/a* alleles as C3H.

provide a more detailed physical map of the region (Fig. 2b). Dinucleotide repeat sequences were identified from draft sequence of the most proximal BAC in the contig, RP23-116J6, which contains the cone-rod homeobox (*Crx*) gene. A SLP, 116J6.1, was identified in one such repeat (Table 1, Fig. 3). Genotyping of recombinant mice reveals that *hyh* lies distal to this marker, localizing the *hyh* gene to this contig between 116J6.1 and *D7Mit56* (Fig. 1), a region spanning approximately 1.6 Mb (Kim et al. 2001).

Gene content of candidate interval. Through limited sequencing of BACs in the contig and analysis of draft sequence of the mouse and human genomes available through NCBI, a number of genes were localized to the *hyh* candidate interval (Fig. 2b). The presence and physical location of the majority of these genes were confirmed by PCR (Table 1) or Southern blot analysis of YAC and BAC clones within the contig. Gene content has since been further confirmed by recently published assembly and annotation of human and mouse sequence encompassing the candidate interval (Dehal et al. 2001; Kim et al. 2001). Genes identified within the candidate interval establish conservation between this region of mouse Chr 7 and human Chr 19q13.3.

Mouse orthologs of the human genes CRX, selenoprotein W 1 (SEPW1), glioma tumor suppressor candidate region protein 2 (GLTSCR2), glioma tumor suppressor candidate region 1 (GLTSCR1), and EH-domain containing protein 2 (EHD2), which fall within the glioma tumor suppressor candidate region on human Chr 19q13.3 (Smith et al. 2000), are all found in the proximal half of the *hyh* candidate interval in the same order as on human Chr 19q13.3. More distally lie a number of other genes: kaptin (*Kaptn*), N-ethylmaleimide sensitive fusion protein attachment protein alpha (*Napa*), solute carrier family 8 (sodium/calcium exchanger)

member 2 (*Slc8a2*), myeloid ecotropic viral integration site-related gene 2 (*Mrg2*), p-53 upregulated modulator of apoptosis (*Puma*), ubiquitin-like 1 activating enzyme E1A (*Uble1a*), *Kiaa1064* and neuronal PAS domain protein 1 (*Npas1*), all mapping to human Chr 19q13.3. With the exception of *Crx*, which is known to cause cone-rod dystrophy in humans (Freund et al. 1997; Swain et al. 1997), the remainder of the genes are viable candidates for the *hyh* gene.

Evaluation of candidate genes. Several genes, including *Gltscr1*, *Ehd2*, and *Kiaa1064*, have been evaluated as candidate genes for *hyh* by Northern blot analysis. Both levels and sizes of transcripts were found to be normal in *hyh* homozygous mutants (data not shown). However, Northern blot analysis detects only a subset of possible mutations and can miss point mutations within the coding sequence that do not affect splice sites or transcript stability. To definitively rule out these genes would require sequencing these loci in *hyh* mice. The coding sequence of *Ehd2* has been analyzed in *hyh/hyh* mice, and no mutations were identified (data not shown).

Genes within the myotonic dystrophy locus were also considered as candidate genes for *hyh*. These genes map to human Chr 19q13.3 and to proximal Chr 7 in mouse. A number of neonatal myotonic dystrophy cases are associated with hydrocephalus (Fox and Gravett 1986; Garcia-Alix et al. 1991). The mutation in myotonic dystrophy is a triplet expansion in the 3' untranslated region of the dystrophin myotonic-protein kinase (DMPK) gene (Fu et al. 1992). Failure of mouse models to fully reproduce the human myotonic dystrophy phenotype led to the hypothesis that the triplet expansion in DMPK could be affecting neighboring genes to cause the multisystemic symptoms of myotonic dystrophy (Groenen and Wieringa 1998). We hypothesized that independent mutations

within the mouse orthologs of these genes may be the cause of *hyh*. We were unable to locate the mouse ortholog of DMPK, dystrophin myotonic kinase (*Dm15*), within our YAC/BAC contig by PCR, but did identify a polymorphic dinucleotide repeat sequence within intron 9, allowing us to genetically map *Dm15* relative to *hyh* within our cross (Table 1, Fig. 3). *Dm15* cosegregated with *D7Mit76*, which maps outside of the *hyh* candidate interval, distal to *D7Mit56* (Fig. 1), making genes within the myotonic dystrophy locus highly unlikely candidates for *hyh*.

Discussion

This study maps the *hyh* gene to a region on Chr 7 bounded proximally by *Crx* and distally by *D7Mit56*. This map position is approximately 13 cM centromeric to the previously published map position of 15.2 cM. *hyh* was originally mapped in a 3-point intercross relative to *Gpil* and the hemoglobin β -chain (*Hbb*) locus (Bronson and Lane 1990) in 80 meioses. *hyh* was positioned distal to *Gpil* by assuming the least number of double crossovers. The new mapping data from a larger cross, analyzing 903 meioses and utilizing more markers, demonstrate that *hyh* in fact lies proximal to *Gpil* at approximately 2 cM on proximal Chr 7.

According to the results of our crosses, *D7Mit56* and *D7Mit75* are separated by a genetic distance of 1.55 cM. The MGD map places *D7Mit75* at 1.7 cM and *D7Mit56* at 2.5 cM, which corresponds to a genetic distance of only 0.8 cM. This discrepancy is probably not statistically significant and may be due to normal variation or variable recombination "hotspots" in different strains. Another source of variable recombination rates between these two markers in different crosses may be a major divergence between *Mus spretus* and *Mus musculus* on proximal Chr 7, suggested by mapping of the chloride channel 4-2 (*Clcn4-2*) gene to the X Chr in *Mus spretus*, but to proximal Chr 7 in C57BL/6J (Rugarli et al. 1995). This may have interfered with recombination on proximal Chr 7 in some crosses, such as the JAX (BSB) and JAX (BSS) crosses, which utilized *Mus spretus* and C57BL/6J, leading to underestimation of the actual genetic distance between markers in this region. If this is the case, our estimate of 1.55 cM may be a more accurate reflection of the real genetic distance between *D7Mit75* and *D7Mit56*.

Our genetic and physical mapping of this region has also served to determine the physical order of 10 microsatellite markers that remain unresolved on the MGD map. While our data largely agree with the MGD map, there are several discrepancies in marker and gene order that reflect the advantage of physical mapping data over a composite linkage map. We also identified a SSLP in *D7Mit342* between the closely related strains C57BL/10J and C3HeB/FeJ-*a/a* and identified three novel markers, 469O12.R, 116J6.1, and *Dm15* that are also polymorphic between these strains by SSLP analysis. These data should be useful to others studying this region of Chr 7.

A number of interesting genes have been identified within the *hyh* candidate interval. CRX, SEPW1, GLTSCR1, GLTSCR2, and EHD2 are genes identified within the conserved region of human Chr 19q13, referred to as the glioma tumor suppressor candidate region (Smith et al. 2000; Pohl et al. 2000). With the exception of CRX, which is known to cause cone-rod dystrophy in humans (Swain et al. 1997; Freund et al. 1997) and a similar phenotype in mouse (Furukawa et al. 1999), these genes remain potential candidates for *hyh*. *Uble1a*, *Puma*, *Napa*, *Kptn*, and *Slc8a2* have been implicated in generally utilized cellular mechanisms and seem unlikely to cause the CNS-specific phenotype of *hyh*.

Mrg2, *Kiaa1064*, and *Npas1* are attractive candidates for *hyh* owing to their expression patterns and/or putative functions. *Mrg2* encodes a Pbx-related homeobox gene shown to play a role in anterior-posterior patterning in the *Xenopus* brain (Dibner et al. 2001; Salzberg et al. 1999; Vlachakis et al. 2001). *Kiaa1064* en-

codes a putative transcription factor with a zinc finger motif and is expressed in embryonic brain, as shown by our Northern analysis, as well as in a variety of other tissues. *Npas1* encodes a bHLH transcription factor selectively expressed in the developing and adult central nervous system (Zhou et al. 1997).

Our preliminary analysis of three candidate genes—*Kiaa1064*, *Ehd2*, and *Gltsr1*—by Northern analysis of *hyh/hyh* embryonic brain has not revealed any alterations in expression of these genes, and sequencing of *Ehd2* cDNA from *hyh/hyh* mice revealed no mutations. These data make *Ehd2* highly unlikely to be the *hyh* gene, but *Kiaa1064* and *Gltsr1* cannot be excluded as candidates for *hyh*.

Remarkably, the *hyh* phenotype looks quite similar to a recently described group of human cortical malformations characterized by agenesis of the corpus callosum with interhemispheric cyst (Barkovich et al. 2001). This set of malformations has been classified into several different types, of which Type 1a bears most resemblance to the *hyh* phenotype. These patients present with macrocephaly, communicating hydrocephalus, agenesis or hypogenesis of the corpus callosum, and a large interhemispheric cyst communicating with the third ventricle and at least one of the lateral ventricles. Whether *hyh* and this human malformation share a genetic basis remains to be seen.

Human Chr 19 is the most gene-rich chromosome in the genome, with an average of 23 genes per Mb (Venter et al. 2001). It is likely that conserved regions of the mouse genome will be similarly gene rich, and this is reflected in our physical mapping data. As would be expected from recent homology maps between human Chr 19 and mouse Chr 7 (Stubbs et al. 1996; Kim et al. 2001; Dehal et al. 2001), gene content and order within the *hyh* candidate interval are preserved between mouse and human, though inverted relative to the centromere. Mouse proximal Chr 7 does mirror the high gene density of human Chr 19 and presents a challenge to those undertaking positional cloning of disease genes in this area. The data presented in this paper clarify marker and gene order in a difficult region of the mouse genome and provide physical mapping data that should be valuable to others studying proximal Chr 7.

Acknowledgments. T.H. Chae was supported by an NIH MSTP fellowship and the Stuart H.Q. & Victoria Quan/Tony Adams Fellowship. K.M. Allen was supported by an NRSA postdoctoral fellowship (MH10691) and the Goldenson/Berenberg Fellowship. This work was supported by grant RO1 NS32457 from the NINDS to C.A. Walsh and grant P40 RR01183 to M.T. Davisson.

References

- Altschul SF, Madden TL, Schaffer AA, Zhang J, Zhang Z et al. (1997) Gapped BLAST and PSI-BLAST: a new generation of protein database search programs. *Nucleic Acids Res* 25, 3389–3402
- Ausubel FM, Brent R, Kingston RE, Moore DD, Seidman JG et al. (1995) *Current Protocols in Molecular Biology*. New York: John Wiley & Sons, Inc.
- Barkovich AJ, Simon EM, Walsh CA (2001) Callosal agenesis with cyst: a better understanding and new classification. *Neurology* 56, 220–227
- Bronson RT, Lane PW (1990) Hydrocephalus with hop gait (*hyh*): a new mutation on chromosome 7 in the mouse. *Brain Res Dev Brain Res* 54, 131–136
- Clark F (1932) Hydrocephalus, a hereditary character in the house mouse. *Proc Natl Acad Sci USA* 18, 654–656
- Dehal P, Predki P, Olsen AS, Kobayashi A, Folta P et al. (2001) Human chromosome 19 and related regions in mouse: conservative and lineage-specific evolution. *Science* 293, 104–111
- Dibner C, Elias S, Frank D (2001) XMeis3 protein activity is required for proper hindbrain patterning in *Xenopus laevis* embryos. *Development* 128, 3415–3426
- Fox GN, Gravett MG (1986) Neonatal myotonic dystrophy associated with prenatal ventriculomegaly. A case report. *J Reprod Med* 31, 729–731
- Freund CL, Gregory-Evans CY, Furukawa T, Papaioannou M, Looser J et

- al. (1997) Cone-rod dystrophy due to mutations in a novel photoreceptor-specific homeobox gene (CRX) essential for maintenance of the photoreceptor. *Cell* 91, 543–553
- Fu YH, Pizzuti A, Fenwick Jr RG, King J, Rajnarayan S et al. (1992) An unstable triplet repeat in a gene related to myotonic muscular dystrophy. *Science* 255, 1256–1258
- Furukawa T, Morrow EM, Li T, Davis FC, Cepko CL (1999) Retinopathy and attenuated circadian entrainment in *Crx*-deficient mice. *Nat Genet* 23, 466–470
- Garcia-Alix A, Cabanas F, Morales C, Pellicer A, Echevarria J et al. (1991) Cerebral abnormalities in congenital myotonic dystrophy. *Pediatr Neurol* 7, 28–32
- Green MC (1970) The developmental effects of congenital hydrocephalus (ch) in the mouse. *Dev Biol* 23, 585–608
- Groenen P, Wieringa B (1998) Expanding complexity in myotonic dystrophy. *Bioessays* 20, 901–912
- Hollander W (1976) Hydrocephalic-polydactyl, a recessive pleiotropic mutant in the mouse, and its location in Chromosome 6. *Iowa State J Res* 51, 13–23
- Jimenez AJ, Tome M, Paez P, Wagner C, Rodriguez S et al. (2001) A programmed ependymal denudation precedes congenital hydrocephalus in the *hyh* mutant mouse. *J Neuropathol Exp Neurol* 60, 1105–1119
- Kim J, Gordon L, Dehal P, Badri H, Christensen M et al. (2001) Homology-driven assembly of a sequence-ready mouse BAC contig map spanning regions related to the 46-Mb gene-rich euchromatic segments of human chromosome 19. *Genomics* 74, 129–141
- Kume T, Deng KY, Winfrey V, Gould DB, Walter MA et al. (1998) The forkhead/winged helix gene *Mfl* is disrupted in the pleiotropic mouse mutation congenital hydrocephalus. *Cell* 93, 985–996
- Lander ES, Linton LM, Birren B, Nasbaum C, Zody MC, et al. (2001) Initial sequencing and analysis of the human genome. *Nature* 409, 860–921
- Nusbaum C, Slonim DK, Harris KL, Birren BW, Steen RG et al. (1999) A YAC-based physical map of the mouse genome. *Nat Genet* 22, 388–393
- Perez-Figares JM, Jimenez AJ, Perez-Martin M, Fernandez-Llebrez P, Cifuentes M et al. (1998) Spontaneous congenital hydrocephalus in the mutant mouse *hyh*. Changes in the ventricular system and the subcommissural organ. *J Neuropathol Exp Neurol* 57, 188–202
- Pohl U, Smith JS, Tachibana I, Ueki K, Lee HK et al. (2000) EHD2, EHD3, and EHD4 encode novel members of a highly conserved family of EH domain-containing proteins. *Genomics* 63, 255–262
- Rozen S, Skaletsky HJ (1998) *Primer3*. Cambridge, Mass.: Whitehead Institute for Biomedical Research
- Rugarli EI, Adler DA, Borsani G, Tsuchiya K, Franco B et al. (1995) Different chromosomal localization of the *Clcn4* gene in *Mus spretus* and C57BL/6J mice. *Nat Genet* 10, 466–471
- Salzberg A, Elias S, Nachaliel N, Bonstein L, Henig C et al. (1999) A Meis family protein caudalizes neural cell fates in *Xenopus*. *Mech Dev* 80, 3–13
- Smit AFA, Green P (2000). *RepeatMasker*.
- Smith JS, Tachibana I, Pohl U, Lee HK, Thanarajasingam U et al. (2000) A transcript map of the chromosome 19q-arm glioma tumor suppressor region. *Genomics* 64, 44–50
- Stubbs L, Carver EA, Shannon ME, Kim J, Geisler J et al. (1996) Detailed comparative map of human chromosome 19q and related regions of the mouse genome. *Genomics* 35, 499–508
- Swain PK, Chen S, Wang QL, Affatigato LM, Coats CL et al. (1997) Mutations in the cone-rod homeobox gene are associated with the cone-rod dystrophy photoreceptor degeneration. *Neuron* 19, 1329–1336
- Venter JC, Adams MD, Myers EW, Li PW, Mural RJ, et al. (2001) The sequence of the human genome. *Science* 291, 1304–1351
- Vlachakis N, Choe SK, Sagerstrom CG (2001) Meis3 synergizes with Pbx4 and Hoxb1b in promoting hindbrain fates in the zebrafish. *Development* 128, 1299–1312
- Ware ML, Fox JW, Gonzalez JL, Davis NM, Lambert de Rouvroit C et al. (1997) Aberrant splicing of a mouse disabled homolog, *mdab1*, in the scrambler mouse. *Neuron* 19, 239–249
- Zhou YD, Barnard M, Tian H, Li X, Ring HZ et al. (1997) Molecular characterization of two mammalian bHLH-PAS domain proteins selectively expressed in the central nervous system. *Proc Natl Acad Sci USA* 94, 713–718